

Short Communication

Probucol is anti-hyperalgesic in a mouse peripheral nerve injury model of neuropathic pain

Rebecca L. Joyce^a, Gareth R. Tibbs^a, J. David Warren^b, Christopher J. Costa^c,
 Kelly Aromolaran^a, R. Lea Sanford^d, Olaf S. Andersen^d, Zhucui Li^b, Guoan Zhang^b, Dianna
 E. Willis^{c,e,*}, Peter A. Goldstein^{a,e,f,*}

^a Dept. of Anesthesiology, 1300 York Ave., Weill Cornell Medicine, New York, NY, USA

^b Dept. of Biochemistry, 413 E. 69th Street, Weill Cornell Medicine, New York, NY, USA

^c Burke Neurological Institute, 785 Mamaroneck Avenue, White Plains, NY, USA

^d Dept. of Physiology & Biophysics, 1300 York Ave., Weill Cornell Medicine, New York, NY, USA

^e Feil Family Brain and Mind Research Institute, Weill Cornell Medicine, NY, USA

^f Dept. of Medicine, Weill Cornell Medicine, New York, NY, USA

ARTICLE INFO

Keywords:

Anti-hyperalgesia
 Alkylphenol
 HCN1
 Ion channel
 Spared nerve injury

ABSTRACT

2,6-di-*tert*-butylphenol (2,6-DTBP) ameliorates mechanical allodynia and thermal hyperalgesia produced by partial sciatic nerve ligation in mice, and selectively inhibits HCN1 channel gating. We hypothesized that the clinically utilized non-anesthetic dimerized congener of 2,6-DTBP, probucol (2,6-di-*tert*-butyl-4-[2-(3,5-di-*tert*-butyl-4-hydroxyphenyl)sulfanylpropan-2-ylsulfanyl]phenol), would relieve the neuropathic phenotype that results from peripheral nerve damage, and that the anti-hyperalgesic efficacy *in vivo* would correlate with HCN1 channel inhibition *in vitro*. A single oral dose of probucol (800 mg/kg) relieved mechanical allodynia and thermal hyperalgesia in a mouse spared-nerve injury neuropathic pain model. While the low aqueous solubility of probucol precluded assessment of its possible interaction with HCN1 channels, our results, in conjunction with recent data demonstrating that probucol reduces lipopolysaccharide-induced mechanical allodynia and thermal hyperalgesia, support the testing/development of probucol as a non-opioid, oral antihyperalgesic albeit one of unknown mechanistic action.

Introduction

Neuropathic pain is characterized by neuronal hyperexcitability and spontaneous activity (Liu et al., 2002; Woolf and Ma, 2007) – properties associated with the current, I_h (Santoro and Shah, 2020; Combe and Gasparini, 2021). I_h is carried by hyperpolarization-activated, cyclic nucleotide-regulated (HCN) channels, a four-isoform family (Biel et al., 2009; Wahl-Schott and Biel, 2009) that assembles as homo- and hetero-

tetramers (with only the HCN2 + HCN3 combination being disfavored (Mistrik et al., 2005)), and are present throughout the nervous system (Moosmang et al., 1999; Notomi and Shigemoto, 2004). Importantly, HCN1 mRNA is present in 94% of human sensory neurons whereas HCN2 is present in only 44%; in mice, HCN1 and HCN2 are present in 71% and 72%, respectively. (Shiers et al., 2020). Consistent with this, HCN1 mRNA is present at ~ 2-fold that of HCN2 in human sensory neuron populations, and ~ 11-fold and ~ 29-fold than those of HCN3

Abbreviations: ACN, acetonitrile; ANTS, 8-aminonaphthalene-1,3,6-trisulfonic acid; BSS, balanced salt solution; BSA, bovine serum albumin; CCI, chronic constriction injury; CFA, Complete Freund's Adjuvant; CXCL1, C-X-C Motif Chemokine Ligand 1; DLS, dynamic light scattering; DRG, dorsal root ganglion; DMEM, Dulbecco's Modified Eagle Medium; DMSO, dimethyl sulfoxide; EtOH, ethanol; FBS, fetal bovine serum; GA, general anesthetic; gA, gramicidin A; IL-1 β , interleukin 1 beta; IL-6, interleukin-6; LC-MS/MS, Liquid chromatography with tandem mass; LUV, large unilamellar vesicle; NF- κ B, nuclear factor kappa B; NIH, National Institutes of Health; RT, room temperature; SNI, spared nerve injury; TNF- α , tumor necrosis factor alpha.

* Corresponding authors at: Dept. of Anesthesiology, Weill Cornell Medicine, 1300 York Avenue, Room A-1050, New York, NY 10065, USA (P.A. Goldstein). Burke Neurological Institute, 785 Mamaroneck Avenue, White Plains, NY 10605, USA (D.E. Willis).

E-mail addresses: rlj60@njms.rutgers.edu (R.L. Joyce), tibbsga@med.cornell.edu (G.R. Tibbs), jdwarren@med.cornell.edu (J. David Warren), chc3012@med.cornell.edu (C.J. Costa), kelly.aromolaran@utah.edu (K. Aromolaran), rls463@med.cornell.edu (R. Lea Sanford), sparre@med.cornell.edu (O.S. Andersen), zh14007@med.cornell.edu (Z. Li), guz2004@med.cornell.edu (G. Zhang), diw2004@med.cornell.edu (D.E. Willis), pag2014@med.cornell.edu (P.A. Goldstein).

<https://doi.org/10.1016/j.ynpai.2023.100141>

Received 16 June 2023; Received in revised form 25 July 2023; Accepted 1 August 2023

Available online 2 August 2023

2452-073X/© 2023 The Authors. Published by Elsevier Inc. This is an open access article under the CC BY-NC-ND license (<http://creativecommons.org/licenses/by-nc-nd/4.0/>).

and HCN4, respectively (North et al., 2019). Electrophysiologic analysis suggests HCN1 is the primary isoform in human sensory neurons (Young et al., 2014).

Post-injury, HCN channel expression and I_h increase in sensory neurons (Chaplan et al., 2003; Yao et al., 2003; Tsuboi et al., 2004; Kitagawa et al., 2006; Luo et al., 2007; Jiang et al., 2008). The increase in HCN expression is greater for HCN1 than for HCN2 (Jiang et al.,

2008), and subunit trafficking is altered (Chaplan et al., 2003; Wells et al., 2007; Jiang et al., 2008), with axonal (not somatic) accumulation of channel protein (Jiang et al., 2008). Increased HCN expression is accompanied by increased I_h amplitude and cellular hyperexcitability (Liu et al., 2002; Chaplan et al., 2003; Tsuboi et al., 2004; Kitagawa et al., 2006), both of which are inhibited by the HCN channel blocker ZD7288 (Chaplan et al., 2003; Yao et al., 2003; Lee et al., 2005; Sun

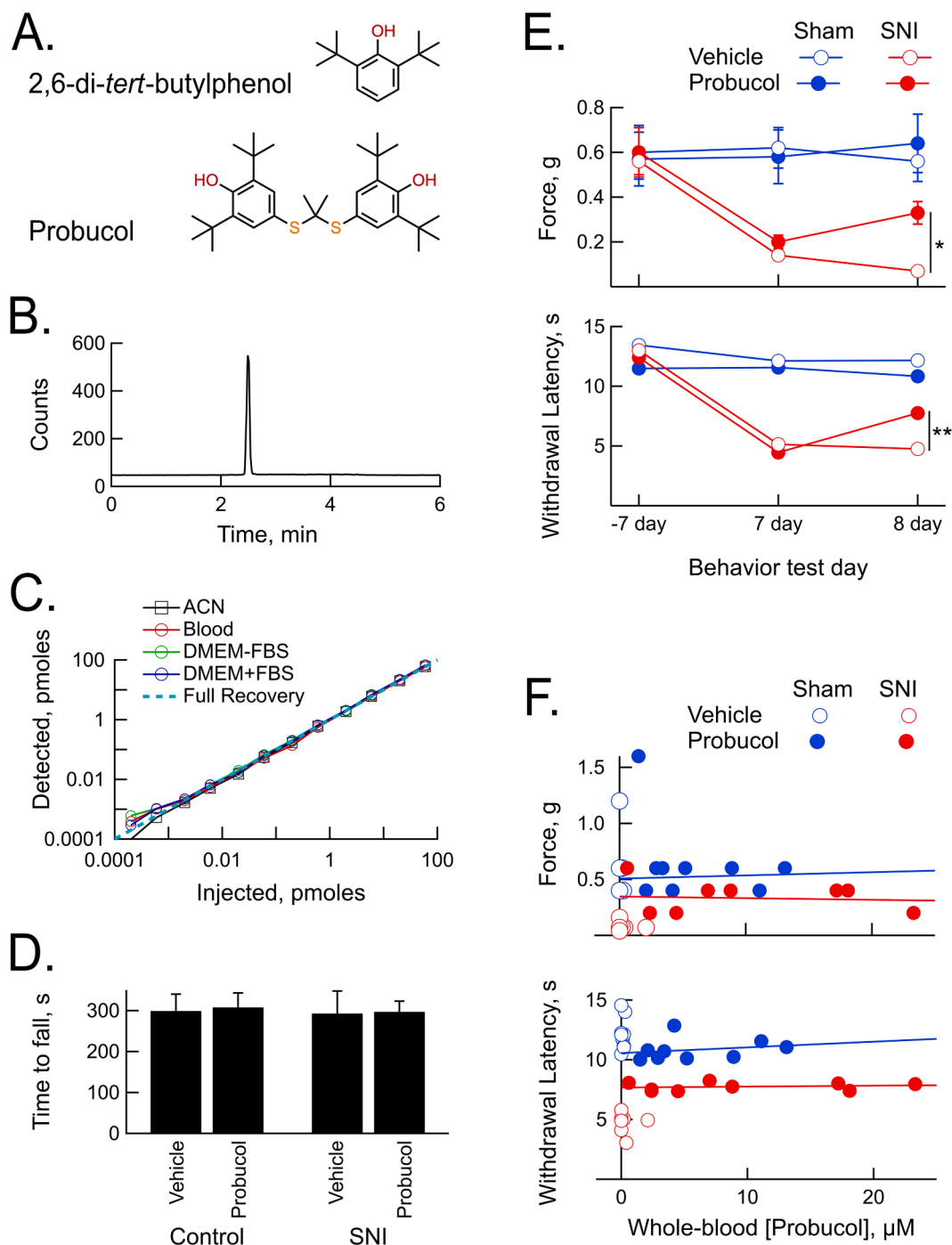


Fig. 1. Probucol attenuates mechanical and thermal hyperalgesia. A. Structures as indicated. B. Representative LC-MS/MS probucol chromatogram. C. Probucol extraction and detection from spiked samples is quantitative. D-F. Groups of mice ($n = 9$ / treatment group) underwent surgery (Day 0), behavioral testing (Day 7, pre-probucol) and, following oral administration of probucol, testing 24 hrs later (Day 8). D. Probucol had no effect on time on rotarod but significantly relieved mechanical allodynia and thermal hyperalgesia (E) (mechanical: $p = 0.0446$ comparing SNI probucol treated vs. SNI vehicle treated at the 8 day timepoint, $t = 2.2054$, $df = 14$ as indicated by *; and thermal: $p = 0.0096$ comparing SNI probucol treated vs. SNI vehicle treated at the 8 day timepoint, $t = 3.0000$, $df = 14$ as indicated by **). F. Antihyperalgesic efficacy was independent of whole-blood concentration. Lines are linear regressions. The plus-probucol sham outlier at 1.6 g in the von Frey data was excluded from the regression.

et al., 2005; Jiang et al., 2008). *Hcn1* or *Hcn2* deletion attenuates different aspects of neuropathic pain (Momin et al., 2008; Orío et al., 2009; Emery et al., 2011; Tsantoulas et al., 2017).

Spontaneous activity in the sciatic nerve ipsilateral to injury is I_h -dependent (Chaplan et al., 2003; Lee et al., 2005; Sun et al., 2005; Jiang et al., 2008), and intraperitoneal (*i.p.*) administration of ZD7288 is antihyperalgesic (Chaplan et al., 2003; Lee et al., 2005; Luo et al., 2007). As *i.p.* administration is not accompanied by CNS accumulation and intrathecal ZD7288 is not antihyperalgesic, peripheral HCN channels appear to be the relevant target (Chaplan et al., 2003; Dalle and Eisenach, 2005; Luo et al., 2007; Jiang et al., 2008).

Previously, we demonstrated that: 1) the intravenous general anesthetic (GA) 2,6-di-*iso*-propylphenol (propofol) preferentially inhibits HCN1 channel gating, with little/no effect on HCN2-4 channels (Cacheaux et al., 2005), 2) subhypnotic doses of propofol relieve mechanical allodynia and thermal hyperalgesia following partial sciatic nerve ligation in mice, and 3) the non-GA 2,6-di-*tert*-butylphenol (2,6-DTBP, Fig. 1A; (James and Glen, 1980; Krasowski et al., 2001)) retains propofol's selectivity for HCN1 over HCN2-4 channels as well as its antihyperalgesic efficacy (Tibbs et al., 2013).

We therefore examined whether the clinically utilized dimerized congener of 2,6-DTBP, probucol (2,6-di-*tert*-butyl-4-[2-(3,5-di-*tert*-butyl-4-hydroxyphenyl)sulfanyl]propan-2-ylsulfanyl]phenol) (Fig. 1A), relieves neuropathic pain-like behaviors, and whether the antihyperalgesic efficacy *in vivo* would correlate with HCN1 channel inhibition *in vitro*.

Material and methods

In vivo experimentation

Animals

To minimize animal use, in this initial survey we considered only adult (30 gm) males. All animal experiments were carried out with institutional approval and in accordance with the NIH guide for the care and use of laboratory animals (NIH Publications No. 8023, revised 1978); all efforts were made to minimize suffering.

Spared nerve injury (SNI) surgery

Animals were randomly assigned to sham-operated and SNI groups; SNI was performed as described (Decosterd and Woolf, 2000; Pertin et al., 2007). Adequacy of anesthetic depth (achieved with isoflurane 1–5%) was determined by loss of corneal reflex and withdrawal to toe pinch.

Drug dosing and behavioral testing

Probuco is very hydrophobic and bioavailability following enteral administration in rats (Heeg et al., 1984) and humans (Heeg and Tachizawa, 1980) is <10% but when delivered *via* oil-solvated gavage (Palin and Wilson, 1984; Fujimura et al., 1992) delivery is efficacious, consistent with drug uptake by the lymphatic system (Han et al., 2016). Following enteral admission, peak plasma levels occur 2–18 h after dosing (Heeg et al., 1984; Palin and Wilson, 1984; Zaitseva et al., 1996), with a mean retention time of 20 – 58 h (Heeg et al., 1984; Zaitseva et al., 1996); following a single dose of probucol (10 mg/kg), the terminal $t_{1/2}$ is 5.6 (oral administration) and 6.1 (intravenous administration) days (Heeg et al., 1984). Thus, conducting the behavioral tests at 24 h following oil-solubilized gavage-dosing is appropriate. Sham and SNI animals (18 animals/group) were each randomly assigned to receive vehicle (peanut oil; 0.5 ml) or probucol (800 mg/kg in 0.5 ml of vehicle) *via* gavage (Palin and Wilson, 1984; Fujimura et al., 1992) once on day 0 (corresponding to seven days post-surgery). All testing was performed at 48 hrs prior to surgery and 24 hrs prior to and following probucol (or vehicle) administration. Blood samples were obtained 24 hrs after completion of testing by exsanguination. Measurements at later time points can be considered in future studies.

To assess mechanical allodynia, a simplified up-down method with von Frey filaments was used to estimate the 50% withdrawal threshold (Chaplan et al. 1994; Dixon 1980). To examine thermal hyperalgesia, we used the Hargreaves method and apparatus (IITC Life Science, Woodland Hills, CA) (Hargreaves et al. 1988), and the radiant heat source intensity was set to evoke a baseline response of 12 s (*i.e.*, 30% intensity, where 100% represents 150 W) (Tibbs et al., 2013). Paw withdrawal latency was calculated as the time between when the desired temperature was reached and the time of withdrawal, shaking or licking of the subject paw. If the paw was not withdrawn within 30 s, the trial was terminated and a latency of 30 s was noted. Motor control was tested using a standard rotarod assay (Karl et al. 2003).

Determination of probucol concentration

Liquid chromatography with tandem mass spectrometry (LC-MS/MS)

LC-MS/MS was performed using a Phenomenex Luna C8(2) column (30 × 2, 5 μ m) at 30 °C, an Agilent 1290 Infinity II UPLC system, and an Agilent 6495 triple quadrupole mass spectrometer in negative electrospray ionization mode. The mobile phase profile was formed by combination of solution A (0.1% formic acid, 10 mM ammonium formate, 60% ACN, 40% H₂O) and solution B (0.1% formic acid with 10 mM ammonium formate, 10% ACN, 90% isopropanol) as follows: 0–2 min 1% B linearly rising to 80% B; 2–3.5 min held at 80% B; 3.5–4 min linearly decreasing to 1% B; 4–6 min held at 1% B. The flow rate was 0.5 ml/min. Multiple reaction monitoring was performed using the transition of m/z of 515.3 → 236.1. The collision energy was 50 V with cell acceleration voltage of 2 V. Recovery and detection of probucol using this method was quantitative in all sample types examined (Fig. 1B,C).

LC-MS/MS sample preparation

After addition of LC-MS/MS-grade acetonitrile (ACN), aliquots of blood (plus citrate anticoagulant), saline or media were vortexed briefly then nutated at 4 °C overnight. Following spin clarification at room temperature (RT), samples were diluted 1:10 into H₂O:ACN and immediately analyzed.

Cell culture, *in vitro* drug delivery, and electrophysiology

HEK293 cells stably transfected with HCN1 were provided by Dr. Stephanie Fenske (LMU München, Pharmakologie für Naturwissenschaften, Germany). Cells were maintained in Gibco DMEM with Glutamax (plus 0.1% glucose and 110 mg/mL sodium pyruvate; ThermoFisher, Cat. #10566016) supplemented with 10% FBS (ThermoFisher, Cat. #A3160402), 1% penicillin/streptomycin (ThermoFisher, Cat. #15140122), and 0.2 mg/ml G418 (ThermoFisher, Cat. #10131035) at 37 °C in a humidified 5% CO₂ incubator. To examine whether probucol altered the function of HCN1 channels, cells were incubated for the indicated time in one of three conditions: basal media (untreated), basal media supplemented with 1% EtOH, or basal media supplemented with 1% EtOH and probucol (33 μ M nominal). Addition of 100 μ l of probucol (3.33 mM or higher in EtOH) to 10 ml of complete media resulted in immediate and obvious drug precipitation. To promote drug:serum protein association, we slowly added 100 μ l of EtOH-solvated probucol (3.33 mM) to 1 ml of undiluted FBS. To this solution, we slowly added 9 ml of DMEM with shaking followed by 20 min sonication at 35 °C; although mildly cloudy, no overt precipitate was observed, suggesting probucol was solubilized or micro-dispersed. Immediately prior to recording, media containing EtOH or EtOH-solvated probucol was replaced with a protein-free extracellular bath solution (2 × washes).

Electrophysiology: Whole-cell patch clamp recordings from single cells were performed at RT and acquired using a Molecular Devices (San Jose, CA) Axopatch 200B amplifier. The 5 kHz output was digitized at 10 kHz using an ITC-18 interface (Instrutech Corp., Port Washington, NY) controlled by Axoclamp software (Molecular Devices). Whole cell

capacity and series resistance compensation was applied with prediction, lag and correction routinely at 80%, 20 μ s, and 95%, respectively. Series resistance was 4–8 M Ω (control 5.6 ± 0.3 , $n = 7$; vehicle 4.7 ± 0.2 , $n = 32$; probucol 6.5 ± 0.6 , $n = 35$).

Patch electrodes (thin-wall borosilicate glass) were coated with Sylgard (Dow Corning Corp., Midland, MI) and had a resistance of 1–2 M Ω when filled with intracellular solution, which contained (in mM): NaCl 10, KCl 130, MgCl₂ 0.5, EGTA 1, HEPES 5, ATP-Mg 3, GTP-Na 0.5, pH 7.4 (with KOH). Extracellular bath contained (in mM): NaCl 110, KCl 30, CaCl₂ 1.8, MgCl₂ 0.5, HEPES 5, pH 7.4 (with NaOH).

Paradigms and analysis: The holding potential was -30 mV. Tail currents were recorded at 0 mV (see (Riegelhaupt et al., 2018) for approach to mitigate collection and analysis bias). Tail current amplitudes were measured in ClampFit; activation curves were fit in IgorPro (Wavemetrics Corporation, Lake Oswego, OR) with the Boltzmann function (where A_1 is the current offset, A_2 the maximal amplitude and V the step voltage):

$$I(V) = A_1 + A_2 / (1 + \exp[(V - V_{1/2})/s]) \quad (1)$$

yielding the activation mid-point ($V_{1/2}$) and slope factor (s , equal to RT/zF where R , T and F have their usual thermodynamic meaning and z is the effective gating valence).

Fluorescence quench measurement of bilayer modification

Large unilamellar vesicles (LUVs), loaded with the disodium salt of 8-aminonaphthalene-1,3,6-trisulfonic acid (ANTS), were prepared from 1,2-dierucoyl-*sn*-glycero-3-phosphocholine using freeze-thawing and extrusion through a 0.1 μ m pore diameter polycarbonate filter. The LUVs were doped with the naturally occurring mixture of gramicidins (gA) from *Bacillus brevis* (gA/lipid mole ratio $\sim 1:2,000$) and DMSO or DMSO-solvated probucol then incubated for 20–24 hrs at 12.5 $^{\circ}$ C. To measure the fluorescence quench rate (at 25 $^{\circ}$ C), the ANTS-loaded LUVs were mixed with Tl^{+} quencher using a stopped-flow spectrofluorometer (SX.20; Applied Photophysics, Surrey, UK); fluorescence quench rate was determined as described (Ingólfsson and Andersen, 2010; Ingólfsson et al., 2010; Tibbs et al., 2013).

Dynamic light scattering (DLS)

To examine probucol solubilization, saline or LUV-containing saline were incubated with probucol for 24 h and then assessed using dynamic light scattering (Anton Paar, Litesizer 500, Graz, Austria).

Data blinding and statistical analysis

In vivo studies

The experimenter performing surgeries and assigning animals to experimental groups was blinded with respect to the baseline (pre-surgical) and post-surgical behavioral profile. A second experimenter, blinded to surgical and drug status, performed the behavioral tests. A third experimenter blinded to all of the above performed the blood analyses and the data analysis. All animals and samples were examined and tabulated prior to unblinding. Data are presented as either scatter plots or mean \pm SD. For continuous behavioral data (Hargreaves) multiple groups were compared by repeated measures ANOVA, followed by Tukey's *post hoc* testing with Bonferroni adjustment for multiple comparisons. Test for mechanical allodynia yield ordinal data and were assessed by Friedman's test with Dunn's *post hoc* test.

In vitro studies

To examine solvation and chemical availability directly, probucol was dispersed at a nominal concentration of 33 μ M into three different media: oocyte bath saline, DMEM, and DMEM supplemented with 10% FBS. To promote equilibration of solvation in a manner that would be

consistent with cell biological analysis, aliquots of media were incubated at 37 $^{\circ}$ C for 6 days. They were then either analyzed directly; filtered through a 0.2 μ m nylon spin filters (VWR 82031–358); or filtered then subjected to dialysis through 10 kDa spin dialysis membranes (Corning Spin-X UF 431478).

Electrophysiologic data were collected and analyzed independently by two experimenters and recordings were randomly selected for independent reanalysis. Data are presented as either scatter plots or mean \pm SD. Tests of significance were performed using Kruskal-Wallis one way analysis of variance on ranks with all pairwise comparisons done using Dunn's method; P value < 0.05 was considered significant.

Chemicals

Salts were from Sigma-Aldrich (St. Louis, MO); ANTS was from Invitrogen/ThermoFisher (Waltham, MA: Cat. #A350); probucol was from Tocris (Minneapolis, MN: Cat. #6199). Stock solutions were prepared in 100% EtOH or DMSO at concentrations up to 300 mM. Visual inspection indicated that EtOH was the preferred vehicle for dispersion into balanced salt solutions (BSSs), but analysis of solvation revealed that, in the absence of protein binding, the free concentration was below the limit of detection (see Results).

Results

3.1 Following a single dose of probucol, there was no evidence of motor impairment (Fig. 1D) but a significant attenuation of mechanical allodynia and thermal hyperalgesia was observed (Fig. 1E). Across all drug-treated mice, the whole blood probucol concentration was 7.6 ± 1.6 μ M ($n = 18$; range [min, max], 0.6, 23.3). Neither the latency before paw withdrawal in response to thermal stimulation nor the force required to elicit withdrawal in response to mechanical stimulation were dependent on the probucol whole-blood concentration across the observed range (Fig. 1F).

3.2 Pilot experiments examining the effect of probucol on gating of HCN1 channels heterologously expressed in *Xenopus* oocytes (*per* our analysis of 2,6-DTBP; (Tibbs et al., 2013)) failed to detect an effect (not shown). Despite reports indicating probucol could be examined at concentrations up to 100 μ M in BSSs (Hayashi et al., 2004; Aubert et al., 2006; Guo et al., 2007; Guo et al., 2011; Taniguchi et al., 2012; Hihara et al., 2013; Zhang et al., 2018; Guo et al., 2023), visual examination of bath solution revealed significant drug precipitation suggesting the absence of an effect could reflect poor bioavailability, not ineffectiveness. Concordantly, in the absence of a high concentration of serum proteins (i.e., oocyte bath saline, DMEM alone) the concentration of solvated probucol was below the limit of detection (~ 3 nM) but in the presence of 10% FBS, probucol is solvated at micromolar concentrations albeit protein bound (Fig. 2A). These data are consistent with the highly hydrophobic nature of probucol (calculated LogP = 10.27; Percepta software v2018.1, ACD Labs, Toronto, Canada) and a previously reported maximal aqueous solubility of 4–10 nM at 25 $^{\circ}$ C (Yagi et al., 1996). Supplementation of oocyte saline with BSA (up to 3% w/v ; (Midwinter et al., 2012)) did not reveal a probucol-effect on HCN1 channel gating suggesting it is stably bound and chemically unavailable during acute (20 min) exposure (data not shown).

3.3 Oocytes are not ideal for chronic exposure experiments; accordingly, we addressed this using HEK293 cells stably transfected with HCN1 and whole-cell patch clamp recordings. Fig. 2B shows current records from two representative whole-cell patch clamp recordings following 6 days in the presence or absence of probucol (nominally 33 μ M). Fig. 2C shows tail current activation curves from these cells and a vehicle control. With prolonged probucol exposure, there was a depolarizing drift in channel gating (Fig. 2D). At days 4–6 the $V_{1/2}$ in the presence of probucol was -60.8 ± 3.38 mV ($n = 17$); corresponding values in control and vehicle were, respectively, -69.8 ± 1.4 mV ($n = 7$) and -69.9 ± 4.7 mV ($n = 21$) ($P < 0.05$, One-way ANOVA - Dunn's

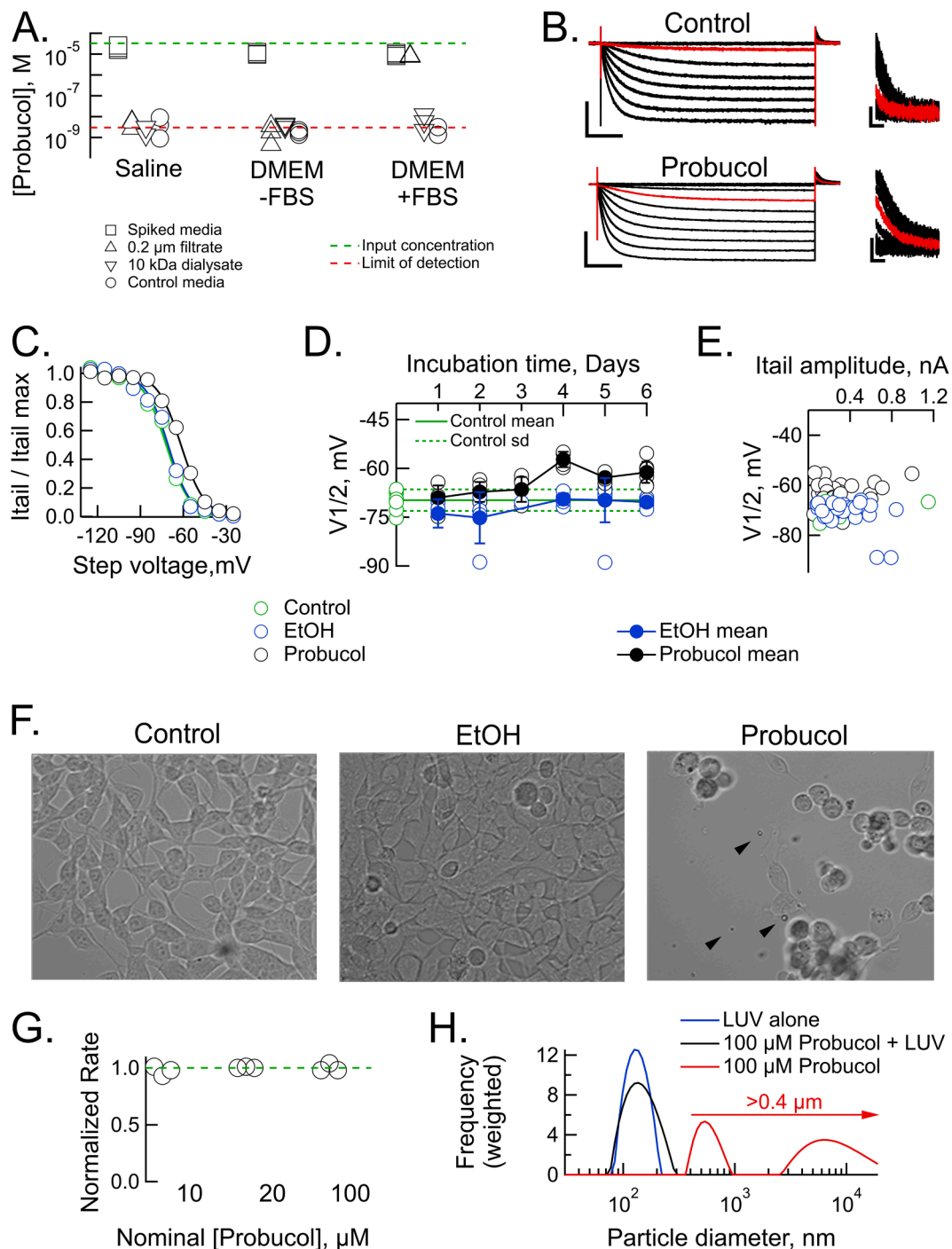


Fig. 2. Probuco solubility is too low to permit examination of acute effects on HCN1 channel function *in vitro*. **A.** Following probuco dispersal at 33 μM (nominal), saline and DMEM (±FBS) samples were equilibrated for 6 days at 37 °C and concentration measured (*per Methods*). **B.** Representative whole cell recordings of HCN1 channels obtained from stably-transfected HEK293 cells following incubation in the absence or presence of probuco (33 μM nominal) in DMEM-10% FBS for 6 days. Records (left) are at voltages between -15 mV and -125 mV (scale bars: 1nA, 500 ms). Records (right) are tail currents at 0 mV (scale bars: 100 pA, 50 ms). Sweeps in red are those obtained with activation at -65 mV. **C.** Normalized activation curves constructed from the cells in **A** plus a vehicle control; smooth lines are fits of the Boltzmann equation. **D.** V_{1/2} as function of days of exposure to DMEM-10% FBS supplemented with either 1% EtOH or 1% EtOH plus probuco (33 μM nominal). **E.** V_{1/2} vs. maximal tail current amplitude. **F.** Photographs of HEK cells stably-transfected with HCN1 following 6 days of culture in basal media or basal media supplemented with 1% EtOH ± probuco (33 μM nominal). Arrowheads highlight small bright and dark flecks in the probuco-treated panel. **G.** Tl⁺ flux as a function of pre-equilibration of LUVs. **H.** Dynamic light scattering intensity as a function of particle size. (For interpretation of the references to colour in this figure legend, the reader is referred to the web version of this article.)

method) but vehicle and control were no different from each other. Series resistance was comparable between the groups (see **Methods**) and there is no marked correlation between current amplitude and V_{1/2} (**Fig. 2E**), suggesting the effect of probuco is not the result of systematic

voltage clamp errors.

3.4 While a modest, anomalous, depolarizing effect on gating cannot be discounted, visual inspection of the cells suggested a more prosaic explanation. After six days in culture with probuco, there was a lower

cell density and a greater number of rounded-up (dead and dying) cells (Fig. 2F). Complete insensitivity of gramicidin-mediated TI^+ flux ($\text{Rate}_{\text{Probuco}}/\text{Rate}_{\text{Control}}$ was 0.97 ± 0.04 , 1.01 ± 0.01 and 1.0 ± 0.03 at nominal concentrations of 10, 20 and 100 μM , respectively) suggests membrane accumulation (if any) does not account for the observed cytotoxicity (Fig. 2G). Importantly, the dynamic light scattering data presented in Fig. 2H show that, in the absence of LUVs, probucol is present as a heterogeneous population of particles of diameter $> 0.4 \mu\text{m}$ but in the presence of LUVs, precipitated probucol is absent, indicating it is fully incorporated into the TI^+ flux LUV membranes. The sizes of the precipitated probucol as determined in the DLS assay is consistent with the near or complete removal of probucol from protein-free solutions by 0.2 μm filtration (Fig. 2A) and the presence of micron-sized bright and dark flecks in the probucol treated cell culture micrograph (Fig. 2F).

Discussion

Probuco is antihyperalgesic in multiple pathologic pain models

Probuco provides rapid antihyperalgesia in a mouse SNI model of neuropathic pain (Fig. 1E). The mechanism of the SNI antihyperalgesia here was examined but not resolved. Does the slow change in HCN1 channel gating upon chronic exposure to probuco exclude a direct drug: channel interaction (Fig. 2)? Probably not. Given the low aqueous solubility (Fig. 2), the effect of the drug could take time to develop due to the slow transfer of drug from the media into the cell and accumulation in hydrophobic compartments in the cell (Gingrich et al., 2009); equally, we cannot rule out that the change in gating is secondary to a slow change in cell physiology. Prolonged incubation in probuco compromised cell viability, which could be indicative of a cellular change that secondarily alters channel gating.

In adult male Swiss mice, probuco (3 mg/kg, oral administration) reduces lipopolysaccharide- and carrageenan-induced mechanical allodynia and thermal hyperalgesia (Zucoloto et al., 2017a; Zucoloto et al., 2017b). These effects were accompanied by reduced leukocyte influx and cytokine production in both paw skin and peritoneum exudate. Interestingly, probuco did not alter lipopolysaccharide-induced tissue oxidative stress at an anti-inflammatory/analgesic dose. Probuco did, however, inhibit lipopolysaccharide-induced NF- κB activation in paw tissue as well as NF- κB activity in cultured macrophages *in vitro* (but note the caveat discussed below regarding *in vitro* drug concentrations); probuco also inhibited carrageenan-induced IL-1 β , TNF- α , and CXCL1 production as well as NF- κB activation (Zucoloto et al., 2017a; Zucoloto et al., 2017b). In mice, probuco (3 mg/kg) also limits Complete Freund's Adjuvant (CFA)-induced changes in neutrophil activity, cytokine levels, as well as NF- κB , microglial, and astrocyte activation (Zucoloto et al., 2019). In the sciatic nerve chronic constriction injury (CCI) neuropathic pain model, probuco – in a dose-dependent manner (8 and 16 mg/kg, oral administration) – significantly relieved thermal hyperalgesia towards both hot and cold stimuli in adult male Sprague Dawley rats; the observed antihyperalgesic effects were accompanied by attenuation of CCI-induced changes in oxidative/nitrosative stress markers (glutathione, malondialdehyde), inflammatory markers [tumor necrosis factor alpha (TNF- α), interleukin-6 (IL-6)], as well as NF- κB /Nlrp3 and Nrf-2 signalling pathways (Derangula et al., 2022). These results indicate that probuco possesses analgesic and anti-inflammatory activities that likely arise from multiple mechanisms. Nonetheless, and irrespective of mechanism, these effects are likely to be peripheral, rather than central, in origin as CNS penetration of probuco is poor (despite its high LogP) (Choisy and Millart, 1980).

In vivo bioavailability

A probuco concentration in whole-blood of $\sim 8 \mu\text{M}$ after a single dose is comparable to the concentration reported 48 h after once daily dosing (800 mg/kg in olive oil) for seven days ($\sim 12 \mu\text{M}$; (Fujimura et al.,

1992)). However, the free concentration is likely no higher than the reported aqueous solubility (4 – 10 nM (Yagi et al., 1996)), with most of the total probuco likely bound to protein and lipid (Urien et al., 1984). As such, the potency of probuco at its antihyperalgesic effector site is uncertain. If probuco acts on a soluble protein it is likely effective at nM concentrations; if, on the other hand, probuco acts on a membrane-embedded protein its actual potency is likely markedly lower (reflecting accumulation in the lipid membrane) albeit that accumulation is not readily apparent in our *in vitro* studies. The lack of a concentration dependence suggests probuco potency is higher than indicated but the delay between the behavioral experiments and the blood draw precludes assessment of its lower limit.

Probuco: In vitro bioavailability

Our observations of micro-dispersed precipitates accords with the reported aqueous solubility of $< 10 \text{ nM}$ (Yagi et al., 1996) and are not consistent with reports that 1–100 μM probuco are readily achievable in aqueous media (Hayashi et al., 2004; Aubert et al., 2006; Guo et al., 2007; Guo et al., 2011; Taniguchi et al., 2012; Hihara et al., 2013; Zucoloto et al., 2017b; Zhang et al., 2018; Guo et al., 2023). Two implications of this finding are: 1) where an effect of acute probuco exposure has been reported, it is likely that probuco has a higher potency than appreciated, and 2) where authors report concentration dependence in the 1–100 μM range, absent demonstration that the drug is solvated and bioavailable, the accuracy of the concentration–response relationship is questionable. While some studies included BSA as an excipient, our experience is that while dispersal of EtOH- or DMSO-solvated probuco into a BSA-rich culture medium may enhance dissolution, but the free concentration is vanishingly small. As such, and given that the exchange between the protein-bound and the free pools is likely very slow, the bound probuco is unlikely to contribute to reported acute experimental effects. As such, the findings presented here raise concerns with regard to earlier cell biological examination of the mechanism of action of probuco.

Conclusions

Our results, along with those demonstrating that probuco can reduce lipopolysaccharide- carrageenan-, and CFA-induced mechanical allodynia and thermal hyperalgesia (Zucoloto et al., 2017a; Zucoloto et al., 2017b; Zucoloto et al., 2019), as well as the neuropathy produced by chronic constriction nerve injury (Derangula et al., 2022), suggest probuco (or its congener, succinobuco (4-[2,6-di-*tert*-butyl-4-[2-(3,5-di-*tert*-butyl-4-hydroxyphenyl)sulfanyl]propan-2-ylsulfanyl]phenoxy]-4-oxobutanoic acid; probuco with a succinate adduct in the 4-position of the second 2,6-DTBP group) may be an effective, non-opioid, oral antihyperalgesic. That probuco can be chronically and safely orally administered to humans (Yamashita and Matsuzawa, 2009) and succinobuco has completed Phase III clinical trials (Tardif et al., 2003; Tardif et al., 2008b; Tardif et al., 2008a) suggests testing either drug could proceed expeditiously.

Declaration of Competing Interest

The authors declare the following financial interests/personal relationships which may be considered as potential competing interests: Peter A. Goldstein reports financial support was provided by US Department of Defense. Olaf A. Andersen reports financial support was provided by National Institutes of Health. Dianna E. Willis reports financial support was provided by National Institutes of Health. Peter A. Goldstein reports a relationship with Akelos, Inc. that includes: board membership and non-financial support. Gareth R. Tibbs reports a relationship with Akelos, Inc. that includes: board membership and non-financial support. Dianna E. Willis reports a relationship with Akelos, Inc. that includes: board membership and non-financial support. J.

David Warren reports a relationship with Akelos, Inc. that includes: board membership and non-financial support. Peter A. Goldstein, Rebecca L. Joyce, and Gareth R. Tibbs are co-inventors on patents related to the development of alkylphenols for the treatment of neuropathic pain. J. David Warren, Dianna E. Willis, Gareth R. Tibbs, and Peter A. Goldstein serve on the Scientific Advisory Board for Akelos, Inc., a research-based biotechnology company that has secured a licensing agreement for the use of those patents.

Acknowledgements

RLJ: methodology, investigation, formal analysis, writing - review; JDW: methodology, investigation, formal analysis, writing - review; CJC: investigation, formal analysis; KA: investigation, formal analysis; RLS: methodology, investigation, formal analysis; OSA: methodology, writing - review; ZL: methodology, investigation, formal analysis, writing - review; GZ: methodology, investigation, formal analysis, writing - review; DEW: conceptualization, data collection, formal analysis, project administration, writing - original draft; writing -review and editing; GRT: conceptualization, data collection, formal analysis, project administration, writing - original draft; writing -review and editing ; PAG: conceptualization, funding acquisition, writing - original draft; writing -review and editing, project administration.

Funding

This work was supported by the U.S. Army Medical Research and Materiel Command [grant number W81XWH1510279], NIH/NINR [NR010797], NIH/NIGMS [GM021342], and the Burke Neurological Institute.

References

- Aubert, M., Osterwalder, R., Wagner, B., Parrilla, I., Cavero, I., Doessegger, L., Ertel, E.A., 2006. Evaluation of the rabbit Purkinje fibre assay as an in vitro tool for assessing the risk of drug-induced torsades de pointes in humans. *Drug Saf.* 29, 237–254. <https://doi.org/10.2165/00002018-200629030-00007>.
- Biel, M., Wahl-Schott, C., Michalak, S., Zong, X., 2009. Hyperpolarization-activated cation channels: from genes to function. *Physiol. Rev.* 89, 847–885. <https://doi.org/10.1152/physrev.00029.2008>.
- Cachaux, L.P., Topf, N., Tibbs, G.R., Schaefer, U.R., Levi, R., Harrison, N.L., Abbott, G. W., Goldstein, P.A., 2005. Impairment of hyperpolarization-activated, cyclic nucleotide-gated channel function by the intravenous general anesthetic propofol. *J. Pharmacol. Exp. Ther.* 315, 517–525. <https://doi.org/10.1124/jpet.105.091801>.
- Chaplan, S.R., Guo, H.Q., Lee, D.H., Luo, L., Liu, C., Kuei, C., Velumian, A.A., Butler, M. P., Brown, S.M., Dubin, A.E., 2003. Neuronal hyperpolarization-activated pacemaker channels drive neuropathic pain. *J. Neurosci.* 23, 1169–1178. <https://doi.org/10.1523/JNEUROSCI.23-04-01169.2003>.
- Choisy, H., Millart, H., 1980. Experimental pharmacology of propracol (author's transl). *La Nouvelle presse medicale* 9, 2981–2984.
- Combe, C.L., Gasparini, S., 2021. Ih from synapses to networks: HCN channel functions and modulation in neurons. *Prog. Biophys. Mol. Biol.* 166, 119–132. <https://doi.org/10.1016/j.pbiomolbio.2021.06.002>.
- Dalle, C., Eisenach, J.C., 2005. Peripheral block of the hyperpolarization-activated cation current (I_h) reduces mechanical allodynia in animal models of postoperative and neuropathic pain. *Reg. Anesth. Pain Med.* 30, 243–248. <https://doi.org/10.1016/j.rapm.2005.01.010>.
- Decosterd, I., Woolf, C.J., 2000. Spared nerve injury: an animal model of persistent peripheral neuropathic pain. *Pain* 87, 149–158. [https://doi.org/10.1016/S0304-3959\(00\)00276-1](https://doi.org/10.1016/S0304-3959(00)00276-1).
- Derangula, K., Javalgekar, M., Kumar Arruri, V., Gundu, C., Kumar Kalvala, A., Kumar, A., 2022. Propracol attenuates NF- κ B/NLRP3 signalling and augments Nrf2 mediated antioxidant defence in nerve injury induced neuropathic pain. *Int. Immunopharmacol.* 102, 108397. <https://doi.org/10.1016/j.intimp.2021.108397>.
- Emery, E.C., Young, G.T., Berrococo, E.M., Chen, L., McNaughton, P.A., 2011. HCN2 ion channels play a central role in inflammatory and neuropathic pain. *Science* 333, 1462–1466. <https://doi.org/10.1126/science.1206243>.
- Fujimura, A., Ohira, H., Ohashi, K., Ebihara, A., 1992. Chronopharmacology of propracol in mice. *Jpn. J. Pharmacol.* 59, 121–124. <https://doi.org/10.1254/jip.59.121>.
- Gingrich, K.J., Burkat, P.M., Roberts, W.A., 2009. Pentobarbital produces activation and block of $\alpha_1\beta_2\gamma_2$ GABA_A receptors in rapidly perfused whole cells and membrane patches: divergent results can be explained by pharmacokinetics. *J. Gen. Physiol.* 133, 171–188. <https://doi.org/10.1085/jgp.200810081>.
- Guo, J., Massaeli, H., Li, W., Xu, J., Luo, T., Shaw, J., Kirshenbaum, L.A., Zhang, S., 2007. Identification of IKr and its trafficking disruption induced by propracol in cultured neonatal rat cardiomyocytes. *J. Pharmacol. Exp. Ther.* 321, 911–920. <https://doi.org/10.1124/jpet.107.120931>.
- Guo, J., Li, X., Shallow, H., Xu, J., Yang, T., Massaeli, H., Li, W., Sun, T., Pierce, G.N., Zhang, S., 2011. Involvement of caveolin in propracol-induced reduction in HERG plasma-membrane expression. *Mol. Pharmacol.* 79, 806–813. <https://doi.org/10.1124/mol.110.069419>.
- Guo, J., Ren, R., Guo, Z., Sun, K., He, J., Shao, J., Wang, X., 2023. Propracol suppresses osteoclastogenesis via activating Nrf2 signaling and ameliorates ovariectomy-induced bone loss. *Int. Immunopharmacol.* 116, 109820. <https://doi.org/10.1016/j.intimp.2023.109820>.
- Han, L., Yang, Q., Shen, T., Qing, J., Wang, J., 2016. Lymphatic transport of orally administered propracol-loaded mPEG-DSPE micelles. *Drug Deliv.* 23, 1955–1961. <https://doi.org/10.3109/10717544.2015.1028600>.
- Hayashi, K., Shimizu, M., Ino, H., Yamaguchi, M., Terai, H., Hoshi, N., Higashida, H., Terashima, N., Uno, Y., Kanaya, H., Mabuchi, H., 2004. Propracol aggravates long QT syndrome associated with a novel missense mutation M124T in the N-terminus of HERG. *Clin. Sci.* 107 (2), 175–182.
- Heeg, J.F., Tachizawa, H., 1980. Plasma levels of propracol in man after single and repeated oral doses (author's transl). *Nouvelle Presse Med* 9, 2990–2994.
- Heeg, J.F., Hiser, M.F., Satonin, D.K., Rose, J.Q., 1984. Pharmacokinetics of propracol in male rats. *J. Pharm. Sci.* 73, 1758–1763. <https://doi.org/10.1002/jps.2600731225>.
- Hihara, T., Taniguchi, T., Ueda, M., Yoshinaga, T., Miyamoto, N., Sawada, K., 2013. Propracol and the cholesterol synthesis inhibitors simvastatin and triparanol regulate I_h channel function differently. *Hum. Exp. Toxicol.* 32, 1028–1037. <https://doi.org/10.1177/0960327112474848>.
- Ingólfsson, H.I., Andersen, O.S., 2010. Screening for small molecules' bilayer-modifying potential using a gramicidin-based fluorescence assay. *Assay Drug Dev Technol* 8, 427–436. <https://doi.org/10.1089/adt.2009.0250>.
- Ingólfsson, H.I., Sanford, R.L., Kapoor, R., Andersen, O.S., 2010. Gramicidin-based fluorescence assay; for determining small molecules potential for modifying lipid bilayer properties. *J Vis Exp* 44:2131. <https://doi.org/10.3791/2131>.
- James, R., Glen, J.B., 1980. Synthesis, biological evaluation, and preliminary structure-activity considerations of a series of alkylphenols as intravenous anesthetic agents. *J. Med. Chem.* 23, 1350–1357. <https://doi.org/10.1021/jm00186a013>.
- Jiang, Y.Q., Xing, G.G., Wang, S.L., Tu, H.Y., Chi, Y.N., Li, J., Liu, F.Y., Han, J.S., Wan, Y., 2008. Axonal accumulation of hyperpolarization-activated cyclic nucleotide-gated cation channels contributes to mechanical allodynia after peripheral nerve injury in rat. *Pain* 137, 495–506. <https://doi.org/10.1016/j.pain.2007.10.011>.
- Kitagawa, J., Takeda, M., Suzuki, I., Kadoi, J., Tsuboi, Y., Honda, K., Matsumoto, S., Nakagawa, H., Tanabe, A., Iwata, K., 2006. Mechanisms involved in modulation of trigeminal primary afferent activity in rats with peripheral mononeuropathy. *Eur. J. Neurosci.* 24 (1976-1986). <https://doi.org/10.1111/j.1460-9568.2006.05065.x>.
- Krasowski, M.D., Jenkins, A., Flood, P., Kung, A.Y., Hopfinger, A.J., Harrison, N.L., 2001. General anesthetic potencies of a series of propofol analogs correlate with potency for potentiation of γ -aminobutyric acid (GABA) current at the GABA_A receptor but not with lipid solubility. *J. Pharmacol. Exp. Ther.* 297, 338–351.
- Lee, D.H., Chang, L., Sorkin, L.S., Chaplan, S.R., 2005. Hyperpolarization-activated, cation-nonselective, cyclic nucleotide-modulated channel blockade alleviates mechanical allodynia and suppresses ectopic discharge in spinal nerve ligated rats. *J. Pain* 6, 417–424. <https://doi.org/10.1016/j.jpain.2005.02.002>.
- Liu, C.N., Devor, M., Waxman, S.G., Kocsis, J.D., 2002. Subthreshold oscillations induced by spinal nerve injury in dissociated muscle and cutaneous afferents of mouse DRG. *J. Neurophysiol.* 87, 2009–2017. <https://doi.org/10.1152/jn.00705.2001>.
- Luo, L., Chang, L., Brown, S.M., Ao, H., Lee, D.H., Higuera, E.S., Dubin, A.E., Chaplan, S. R., 2007. Role of peripheral hyperpolarization-activated cyclic nucleotide-modulated channel pacemaker channels in acute and chronic pain models in the rat. *Neuroscience* 144, 1477–1485. <https://doi.org/10.1016/j.neuroscience.2006.10.048>.
- Midwinter, R.G., Maghzal, G.J., Dennis, J.M., Wu, B.J., Cai, H., Kapralov, A.A., Belikova, N.A., Tyurina, Y.Y., Dong, L.F., Khachigian, L., Neuzil, J., Kagan, V.E., Stocker, R., 2012. Succinobucol induces apoptosis in vascular smooth muscle cells. *Free Radic. Biol. Med.* 52, 871–879. <https://doi.org/10.1016/j.freeradbiomed.2011.11.029>.
- Mistrik, P., Mader, R., Michalak, S., Weidinger, M., Pfeifer, A., Biel, M., 2005. The murine HCN3 gene encodes a hyperpolarization-activated cation channel with slow kinetics and unique response to cyclic nucleotides. *J. Biol. Chem.* 280, 27056–27061. <https://doi.org/10.1074/jbc.M502696200>.
- Momin, A., Cadiou, H., Mason, A., McNaughton, P.A., 2008. Role of the hyperpolarization-activated current I_h in somatosensory neurons. *J. Physiol.* 586, 5911–5929. <https://doi.org/10.1113/jphysiol.2008.163154>.
- Moosmang, S., Biel, M., Hofmann, F., Ludwig, A., 1999. Differential distribution of four hyperpolarization-activated cation channels in mouse brain. *Biol. Chem.* 380, 975–980. <https://doi.org/10.1515/BC.1999.121>.
- North, R.Y., Li, Y., Ray, P., Rhines, L.D., Tatsui, C.E., Rao, G., Johansson, C.A., Zhang, H., Kim, Y.H., Zhang, B., Dussor, G., Kim, T.H., Price, T.J., Dougherty, P.M., 2019. Electrophysiological and transcriptomic correlates of neuropathic pain in human dorsal root ganglion neurons. *Brain* 142, 1215–1226. <https://doi.org/10.1093/brain/awz063>.
- Notomi, T., Shigemoto, R., 2004. Immunohistochemical localization of I_h channel subunits, HCN1–4, in the rat brain. *J Comp Neurol* 471, 241–276. <https://doi.org/10.1002/cne.11039>.
- Orio, P., Madrid, R., de la Peña, E., Parra, A., Meseguer, V., Bayliss, D.A., Belmonte, C., Viana, F., 2009. Characteristics and physiological role of hyperpolarization activated currents in mouse cold thermoreceptors. *J. Physiol.* 587, 1961–1976. <https://doi.org/10.1113/jphysiol.2008.165738>.

- Palin, K.J., Wilson, C.G., 1984. The effect of different oils on the absorption of probucol in the rat. *J. Pharm. Pharmacol.* 36, 641–643. <https://doi.org/10.1111/j.2042-7158.1984.tb04919.x>.
- Pertin, M., Allchorne, A.J., Beggah, A.T., Woolf, C.J., Decosterd, I., 2007. Delayed sympathetic dependence in the spared nerve injury (SNI) model of neuropathic pain. *Mol. Pain* 3, 21. <https://doi.org/10.1186/1744-8069-3-21>.
- Riegelhaupt, P.M., Tibbs, G.R., Goldstein, P.A., 2018. HCN and K_{DP} Channels in Anesthetic Mechanisms Research. *Methods Enzymol.* 602, 391–416. <https://doi.org/10.1016/bs.mie.2018.01.015>.
- Santoro, B., Shah, M.M., 2020. Hyperpolarization-Activated Cyclic Nucleotide-Gated Channels as Drug Targets for Neurological Disorders. *Annu. Rev. Pharmacol. Toxicol.* 60, 109–131. <https://doi.org/10.1146/annurev-pharmtox-010919-023356>.
- Shiers, S., Klein, R.M., Price, T.J., 2020. Quantitative differences in neuronal subpopulations between mouse and human dorsal root ganglia demonstrated with RNAscope in situ hybridization. *Pain* 161, 2410–2424. <https://doi.org/10.1097/j.pain.0000000000001973>.
- Sun, Q., Xing, G.G., Tu, H.Y., Han, J.S., Wan, Y., 2005. Inhibition of hyperpolarization-activated current by ZD7288 suppresses ectopic discharges of injured dorsal root ganglion neurons in a rat model of neuropathic pain. *Brain Res.* 1032, 63–69. <https://doi.org/10.1016/j.brainres.2004.10.033>.
- Taniguchi, T., Uesugi, M., Arai, T., Yoshinaga, T., Miyamoto, N., Sawada, K., 2012. Chronic probucol treatment decreases the slow component of the delayed-rectifier potassium current in CHO cells transfected with KCNQ1 and KCNE1: a novel mechanism of QT prolongation. *J. Cardiovasc. Pharmacol.* 59, 377–386. <https://doi.org/10.1097/FJC.0b013e318245e0c5>.
- Tardif, J.C., Gregoire, J., Schwartz, L., Tittle, L., Laramée, L., Reeves, F., Lesperance, J., Bourassa, M.G., L'Allier, P.L., Glass, M., Lambert, J., Guertin, M.C., 2003. Effects of AGI-1067 and probucol after percutaneous coronary interventions. *Circulation* 107, 552–558. <https://doi.org/10.1161/01.cir.0000047525.58618.3c>.
- Tardif, J.C., McMurray, J.J., Klug, E., Small, R., Schumi, J., Choi, J., Cooper, J., Scott, R., Lewis, E.F., L'Allier, P.L., Pfeffer, M.A., 2008a. Effects of succinobucol (AGI-1067) after an acute coronary syndrome: a randomised, double-blind, placebo-controlled trial. *Lancet* 371, 1761–1768. [https://doi.org/10.1016/S0140-6736\(08\)60763-1](https://doi.org/10.1016/S0140-6736(08)60763-1).
- Tardif, J.C., Gregoire, J., L'Allier, P.L., Ibrahim, R., Anderson, T.J., Reeves, F., Tittle, L.M., Schampaert, E., LeMay, M., Lesperance, J., Scott, R., Guertin, M.C., Brennan, M.L., Hazen, S.L., Bertrand, O.F., 2008b. Effects of the antioxidant succinobucol (AGI-1067) on human atherosclerosis in a randomized clinical trial. *Atherosclerosis* 197, 480–486. <https://doi.org/10.1016/j.atherosclerosis.2006.11.039>.
- Tibbs, G.R., Rowley, T.J., Sanford, R.L., Herold, K.F., Proekt, A., Hemmings, H.C., Andersen, O.S., Goldstein, P.A., Flood, P.D., 2013. HCN1 channels as targets for anesthetic and non-anesthetic propofol analogs in the amelioration of mechanical and thermal hyperalgesia in a mouse model of neuropathic pain. *J. Pharmacol. Exp. Ther.* 345 (3), 363–373.
- Tsantoulas C, Lafnéz S, Wong S, Mehta I, Vilar B, McNaughton PA (2017) Hyperpolarization-activated cyclic nucleotide-gated 2 (HCN2) channels drive pain in mouse models of diabetic neuropathy. *Sci Transl Med* 9:eaam6072. DOI: 10.1126/scitranslmed.aam6072.
- Tsuboi, Y., Takeda, M., Tanimoto, T., Ikeda, M., Matsumoto, S., Kitagawa, J., Teramoto, K., Simizu, K., Yamazaki, Y., Shima, A., Ren, K., Iwata, K., 2004. Alteration of the second branch of the trigeminal nerve activity following inferior alveolar nerve transection in rats. *Pain* 111, 323–334. <https://doi.org/10.1016/j.pain.2004.07.014>.
- Urien, S., Riant, P., Albengres, E., Brioude, R., Tillement, J.P., 1984. *In vitro* studies on the distribution of probucol among human plasma lipoproteins. *Mol. Pharmacol.* 26, 322–327.
- Wahl-Schott, C., Biel, M., 2009. HCN channels: structure, cellular regulation and physiological function. *Cell. Mol. Life Sci.* 66, 470–494. <https://doi.org/10.1007/s00018-008-8525-0>.
- Wells, J.E., Rowland, K.C., Proctor, E.K., 2007. Hyperpolarization-activated channels in trigeminal ganglia innervating healthy and pulp-exposed teeth. *Int. Endod. J.* 40, 715–721. <https://doi.org/10.1111/j.1365-2591.2007.01297.x>.
- Woolf, C.J., Ma, Q., 2007. Nociceptors—noxious stimulus detectors. *Neuron* 55, 353–364. <https://doi.org/10.1016/j.neuron.2007.07.016>.
- Yagi, N., Terashima, Y., Kenmotsu, H., Sekikawa, H., Takada, M., 1996. Dissolution behavior of probucol from solid dispersion systems of probucol-polyvinylpyrrolidone. *Chem. Pharm. Bull.* 44 (1), 241–244.
- Yamashita, S., Matsuzawa, Y., 2009. Where are we with probucol: a new life for an old drug? *Atherosclerosis* 207, 16–23. <https://doi.org/10.1016/j.atherosclerosis.2009.04.002>.
- Yao, H., Donnelly, D.F., Ma, C., LaMotte, R.H., 2003. Upregulation of the hyperpolarization-activated cation current after chronic compression of the dorsal root ganglion. *J. Neurosci.* 23, 2069–2074. <https://doi.org/10.1523/JNEUROSCI.23-06-02069.2003>.
- Young, G.T., Gutteridge, A., Fox, H.D., Wilbrey, A.L., Cao, L., Cho, L.T., Brown, A.R., Benn, C.L., Kammonen, L.R., Friedman, J.H., Bictash, M., Whiting, P., Bilsland, J.G., Stevens, E.B., 2014. Characterizing human stem cell-derived sensory neurons at the single-cell level reveals their ion channel expression and utility in pain research. *Mol. Ther.* 22, 1530–1543. <https://doi.org/10.1038/mt.2014.86>.
- Zaitseva, T.M., Dobrotvorskii, A.E., Titov, V.N., Poluéktova, V.P., Gabova, L.V., Smirnov, L.D., 1996. PHARMACOKINETICS OF WATER-SOLUBLE AND INSOLUBLE FORMS OF PROBUCOL. *Pharmaceut Chem J* 30 (12), 731–733.
- Zhang, M., Hou, Y., Shen, Y., Guo, X., Shang, D., Zhang, D., 2018. Probucol reverses homocysteine induced inflammatory monocytes differentiation and oxidative stress. *Eur. J. Pharmacol.* 818, 67–73. <https://doi.org/10.1016/j.ejphar.2017.10.030>.
- Zucoloto, A.Z., Manchope, M.F., Staurengo-Ferrari, L., Alves-Filho, J.C., Cunha, T.M., Antunes, M.M., Menezes, G.B., Cunha, F.Q., Casagrande, R., Verri Jr., W.A., 2017a. Probucol attenuates overt pain-like behavior and carrageenan-induced inflammatory hyperalgesia and leukocyte recruitment by inhibiting NF-KB activation and cytokine production without antioxidant effects. *Inflammation research : official journal of the European Histamine Research Society [et al]* 66, 591–602. <https://doi.org/10.1007/s00011-017-1040-8>.
- Zucoloto, A.Z., Manchope, M.F., Staurengo-Ferrari, L., Pinho-Ribeiro, F.A., Zarpelon, A. C., Saraiva, A.L.L., Cecilio, N.T., Alves-Filho, J.C., Cunha, T.M., Menezes, G.B., Cunha, F.Q., Casagrande, R., Verri Jr., W.A., 2017b. Probucol attenuates lipopolysaccharide-induced leukocyte recruitment and inflammatory hyperalgesia: effect on NF-KB activation and cytokine reduction. *Eur. J. Pharmacol.* 809, 52–63. <https://doi.org/10.1016/j.ejphar.2017.05.016>.
- Zucoloto, A.Z., Manchope, M.F., Borghi, S.M., Dos Santos, T.S., Fattori, V., Badaró-Garcia, S., Camilios-Neto, D., Casagrande, R., Verri Jr., W.A., 2019. Probucol Ameliorates Complete Freund's Adjuvant-Induced Hyperalgesia by Targeting Peripheral and Spinal Cord Inflammation. *Inflammation* 42, 1474–1490. <https://doi.org/10.1007/s10753-019-01011-3>.